Turkish Journal of Science & Technology
18(2), 331-344, 2023.

Research Paper
https://doi.org/10.55525/tjst.1252420

The Effect of Super Resolution Method on Classification Performance of Satellite Images

Ayşe CENGİZ[1], Derya AVCI[2*]
[1] Institute of Science and Technology, Firat University, Elazig, Turkey
[2] Technical Sciences Department of Computer Technology, Firat University, Elazig, Turkey
[1] aayscengiz@gmail.com , *[2] davci@firat.edu.tr

(Geliş/Received: 17/02/2023; Kabul/Accepted: 27/07/2023)

Abstract: The high resolution of the image is very important for applications. Publicly available satellite images generally have low resolutions. Since low resolution causes loss of information, the desired performance cannot be achieved depending on the type of problem studied in the field of remote sensing. In such a case, super resolution algorithms are used to render low resolution images high resolution. Super resolution algorithms are used to obtain high resolution images from low resolution images. In studies with satellite images, the use of images enhanced with super resolution is important. Since the resolution of satellite images is low, the success rate in the classification process is low. In this study, super resolution method is proposed to increase the classification performance of satellite images. The attributes of satellite images were extracted using AlexNet, ResNet50, Vgg19 from deep learning architecture. Then the extracted features were then classified into 6 classes by giving input to AlexNet-Softmax, ResNet50-Softmax, Vgg19-Softmax, Support Vector Machine, K-Nearest Neighbor, decision trees and Naive Bayes classification algorithms. Without super resolution and with super resolution feature extraction and classification processes were performed separately. Classification results without super resolution and with super resolution were compared. Improvement in classification performance was observed using super resolution.

Key words: Super Resolution, Convolutional Neural Networks, Deep Learning, Classification.

Süper Çözünürlük Yönteminin Uydu İmgelerinin Sınıflandırma Performansına Etkisi

Öz: Görüntünün yüksek çözünürlüğü uygulamalar için çok önemlidir. Halka açık sunulan uydu görüntülerinin çözünürlükleri genellikle düşüktür. Düşük çözünürlük bilgi kaybına yol açtığından uzaktan algılama alanında çalışılan problemin türüne bağlı olarak istenilen başarım sağlanamamaktadır. Böyle bir durumda düşük çözünürlüklü görüntülerden yüksek çözünürlüklü görüntü elde etmek için süper-çözünürlük algoritmaları kullanılmaktadır. Uydu görüntüleri ile yapılan çalışmalarda süper çözünürlükle zenginleştirilmiş görüntülerin kullanılması önemlidir. Uydu görüntülerinin çözünürlükleri düşük olduğundan dolayı sınıflandırma işleminde başarım oranı düşük çıkmaktadır. Bu çalışmada, uydu görüntülerinin sınıflandırma başarımını artırmak için süper çözünürlük yöntemi önerilmiştir. Derin öğrenme mimarisinden AlexNet, ResNet50, Vgg19 kullanılarak uydu imgelerinin öznitelikleri çıkarılmıştır. Ardından çıkarılan öznitelikler, AlexNet-Softmax, ResNet50-Softmax, Vgg19-Softmax, Destek Vektör Makinesi, K- En Yakın Komşu ve Naive Bayes sınıflandırma algoritmalarının girişine verilerek 6 sınıfa ayrılmıştır. Süper çözünürlük öncesi ve süper çözünürlük sonrası özellik çıkarma ve sınıflandırma işlemleri ayrı ayrı yapılmıştır. Süper çözünürlükten önce ve sonra sınıflandırma sonuçları karşılaştırılmıştır. Süper çözünürlük kullanılarak sınıflandırma performansında iyileşme gözlemlenmiştir.

Anahtar kelimeler: Süper Çözünürlük, Evrişimsel Sinir Ağları, Derin Öğrenme, Sınıflandırma

1. Introduction

Today, satellite images are actively used in many fields such as address inquiry, field investigation, city planning, agriculture. A large amount of high-resolution (HR) satellite images that enable topographic measurements of the Earth have been obtained by satellites. However, high spatial resolution satellite images present many problems in image classification. With the increase in spatial resolution, more and more details found on the earth's surface appear in satellite images. Objects in the same type of scenes can be seen at different scales and orientations between HR images. When zooming in on satellite images, it is difficult to obtain a clear image because the resolution decreases, and good performance cannot be obtained when classification is made, since the image quality is reduced at low resolution (LR). Super resolution (SR) is a method of obtaining HR images from one or more LR versions of the same image SR has high pixel density. The rate of correct classification of images with increasing resolution increases [1].

In recent years, many new algorithms based on HR image reconstruction [2-5], instance-based [6-8], regression-based [9-11] and deep learning [12-15] have been proposed. One of the main approaches for single

* Corresponding author: davci@firat.edu.tr. ORCID Number of authors: [1] 0000-0003-3829-3243, [2] 0000-0002-5204-0501

frame SR of the image is the interpolation of the image, in which the high frequency information is extracted from the low frequency image and the estimation is made for the detailed information in the first image [16].
There are many methods based on standard interpolation techniques (pixel replication, bilinear, bi-cubic, linear interpolation) that increase the number of pixels without adding details for SR [17-21]. According to image priorities, single image SR algorithms can be categorized into four types. These are prediction models, edge-based methods, image statistical methods and sample-based methods [22-24]. Among them, instance-based methods [25-27] achieve improved performance. Internal instance-based methods take advantage of self-similarity and generate sample patches from the input image. Firstly, Glasner et al. in the study [28], some improved variants are suggested to speed up the implementation. External instance-based methods [29-32] learn from external datasets between low/high resolution patches. SR is applied using multiple images or single images in the frequency domain or spatial domain [33].

SR studies started before deep learning [34]. Advances in deep learning have affected SR studies and successful results have been observed [35-38]. Deep learning-based methods can be grouped according to the type of network architecture, the type of error function used, and different learning principles [39]. Deep learning-based SR is a class of techniques that use deep neural networks to learn the mapping between LR images and their corresponding HR images. The basic idea is to train a deep neural network using a large set of HR and LR image pairs. The network is then used to predict the HR image from the LR input image. Deep learning-based SR methods use convolutional neural networks (CNNs) to learn the mapping between LR and HR images. These methods can improve the accuracy and efficiency of SR, and they have become the state-of-the-art for SR tasks [40,41]. Recurrent Neural Network (RNN), Long Short Term Memory (LSTM), Convolutional Neural Networks (CNN), Generative Adversarial Networks (GAN), Gated Recurrent Unit (GRU) are frequently used deep learning models [42]. In the literature, there are studies in which RNN [43], LSTM [44], CNN [45], GAN [46] network architectures and SR method are used together.

Deep learning-based SR has several applications in computer vision. One of the most popular applications is in the field of image and video processing [47]. SR techniques can be used to improve the resolution of LR images and videos, making them more suitable for various applications such as surveillance [48], medical imaging [49], and remote sensing [50].

Single Image Super-Resolution (SISR) is a technique used in computer vision and image processing to enhance the resolution and quality of a single LR image. The goal of SISR is to generate a HR image from its LR counterpart by inferring the missing high-frequency information [51]. SISR techniques primarily rely on deep learning methods, with convolutional neural networks (CNNs) being widely employed for this task. CNN models are trained on large datasets consisting of paired LR and HR images. The LR images are used as input, while the corresponding HR images serve as ground truth. During the training phase, the CNN model learns to extract relevant features from LR images and generate HR outputs. The optimization objective is to minimize the difference between the generated HR image and the ground truth. This training process enables the model to learn the mapping between LR and HR images, capturing fine details and structures [52]. SISR techniques have significant applications in enhancing the quality of LR images captured from digital cameras or video footage. By upscaling these images, details and textures can be enhanced, resulting in visually improved images [53]. In the medical field, SISR plays a vital role in improving the resolution of medical images, such as MRI or CT scans. HR images facilitate better diagnosis, analysis, and treatment planning, leading to improved patient care [54]. SISR is crucial for improving the resolution of satellite or aerial imagery used in various applications, including surveillance, mapping, and urban planning. HR imagery aids in better understanding and decision-making processes [55].

The classification of satellite imagery has been investigated in the literature. Many studies have focused on the accuracy of classification. Kadhim et al. [56] proposed CNN architectures, namely AlexNet, VGG19, GoogLeNet and Resnet50, to improve the performance of satellite image classification. They compared all the results of the models on three datasets, SAT 4, SAT6 and UCMD. Basu et al. [57] proposed the "DeepSat" method for classification of satellite images. They achieved an accuracy of 97.946 by classifying based on deep unsupervised learning with Convolutional Neural Networks. Albert et al. [58] analyzed land use patterns in urban neighborhoods with state-of-the-art computer vision techniques based on deep convolutional neural networks using satellite images. Robinson et al. [59] proposed a deep learning convolutional neural network model for generating HR population estimates from satellite images. The proposed model demonstrated how machine learning techniques can be an effective tool for extracting information from remotely sensed data. Unnikrishnan et al. [60] proposed three different network architectures (AlexNet, ConvNet, VGG) for the classification of SAT-4 and SAT-6 datasets of satellite images. The proposed models demonstrated the performance of comparative deep learning architectures for high accuracy satellite image classification with fewer trainable parameters. Özbay et al.

[61] analyzed the classification performance of deep learning models in satellite image analysis. They used MobileNetV2, DenseNet201 and ResNet50 architectures as feature extractors. They used convolutional neural network (CNN) models and neighborhood component analysis (NCA) together to manage the classification process more efficiently. The success rate of satellite image classification was 96.46%.

In this study, SR method was proposed to increase the resolution of satellite images and with SR enhanced images were analyzed. Deep learning-based convolutional neural networks are used to make applications such as building detection over enhanced images. Satellite images usually have LR. Therefore, the success rate in the classification process is low. An increase in classification performance was observed with SR.

The organization of this article is as follows: In Chapter 2, information about SR is presented. In Chapter 3, Material and Method is presented. Experimental Results and Discussion is described in Chapter 4. In Chapter 5, Conclusion is presented.

2. Super Resolution

There are two key elements that need to be resolved in SR rendering algorithm. First, all images must be aligned correctly and on top of each other on a common base. The second is to create a new image with higher resolution from these images. If any of these two steps is done incorrectly, no resolution gain can be obtained and the resulting image will not be of the desired quality.

SR in image is the process of recovering HR images from LR images. SR is an important technique used in image processing. SR is used in many fields such as medical imaging [62], satellite imaging [63-65], surveillance and security [66-68], astronomical imaging [69], military imaging [70]. It can be observed that there are some minor differences when using LR images. However, the same LR image cannot be reused when obtaining LR images.

The most common Mean Square Error (MSE), Peak Signal to Noise Ratio(PSNR), Structural Similarity Index Measure (SSIM) metrics are used to measure the performance of models. MSE is the mean squared error. It has been the basis of image quality measurement. Generally, the original image is assumed to be free of any distortion, while the other image is assumed to be contaminated with noise or some other type of error. The difference between them is called the error signal [71].

MSE is a measure of the average squared difference between the pixel values of two images. It is commonly used as a metric to quantify the dissimilarity between an original image and a reconstructed image. The formula to calculate MSE is as follows:

$$MSE=\frac{1}{MxN}\sum_{i=1}^{M}\sum_{j=1}^{N}(X_{ij}-Y_{ij})^2 \quad (1)$$

In the formula, M and N are the dimensions of the images (typically width and height), X(i,j) is the pixel value of the original image at position (i, j), Y(i,j) is the pixel value of the reconstructed image at position (i, j), Σ denotes the sum over all pixels in the image. (X(i,j) - Y(i,j))2 represents the squared difference between the pixel values at corresponding positions (i, j) in the original and reconstructed images.

PSNR is the peak signal to noise ratio. Generally, PSNR is used in image processing. PSNR is more useful than MSE only when comparing images in different dynamic ranges, otherwise equivalent to MSE. The correct range of values for PSNR is typically from 0 to infinity [71]. PSNR is expressed in decibels (dB), and higher PSNR values indicate better quality or higher similarity between two signals or images. The PSNR value is calculated based on the MSE between two signals or images. The MSE is first computed, and then it is used in the PSNR formula to derive the value. C is the maximum possible pixel value of the image data.

$$\text{PSNR}=10*\log_{10}\frac{C_{max}^2}{MSE} \quad (2)$$

Structural Similarity (SSIM) is used to compare the perceptual quality of two images with the mean.

$$SSIM(x,y)=\frac{(2\mu_x\mu_y+c_1)(2\sigma_{xy}+c_2)}{(\mu_x^2+\mu_y^2+c_1)(\sigma_x+\sigma_y+c_2)} \quad (3)$$

In equality, μ_x: mean of X, μ_y: mean of Y, σ_x: variance of X, 2 σ y: variance of Y, σ xy : covariance of X and Y [72].

SR algorithms are techniques used to enhance the resolution and level of detail in digital images or videos. They aim to generate HR versions of LR images by utilizing various computational methods and statistical models. These algorithms have found applications in several domains, including computer vision, image processing, medical imaging, surveillance, and remote sensing.

Single-Image Super-Resolution (SISR) algorithm is used in this study. SISR refers to the task of enhancing the resolution of a single LR image to obtain a HR version. This branch of SR focuses on improving the level of detail, sharpness, and overall visual quality of an image without relying on additional images or frames. SISR algorithms utilize various techniques to infer the missing high-frequency details in a LR image. SISR algorithms find applications in various fields, including digital photography, surveillance systems, medical imaging, satellite imaging, and more. They are used to enhance image quality, support image analysis tasks, improve visualization, and facilitate better decision-making based on HR information.

Algorithim showing the basic steps of SISR algorithm is shown below. Input: The LR image is provided as the input to the algorithm.

1. Preprocessing: Optional preprocessing steps may be applied, such as noise reduction, contrast adjustment, or color space conversion, to improve the quality of the input image.

2. Feature Extraction: Extract relevant features from the LR image. This step involves capturing low-level and high-level features that will help in understanding the image content and structure.

3. SR Network: Train the network using a dataset of LR and corresponding HR image pairs. The network learns the mapping between LR and HR images.

4. Image Reconstruction: Feed the LR image through the trained SR network to generate an initial HR image. The network's architecture and parameters determine how the upsampling and detail enhancement are performed.

5. Post-processing: Apply post-processing techniques to refine the initial HR image. Common post-processing steps include denoising, sharpening, texture enhancement, and artifact reduction.

6. Output: The final output of the SISR algorithm is the enhanced HR image.

3. Material and Method

Since the resolution of satellite images is low, the success rate in the classification process is low. The SR method is proposed to improve the classification performance of satellite images. The main objective of this study is to improve the classification performance of satellite images by using deep learning based SR method to classify satellite images. While determining the main classes, satellite images were used and a total of 6 classes were determined, including mosque, home, hospital, school, park and stadium, which have distinctive features. In order to see the effects of classification performance, the data set was collected manually using Google Earth [73], which has 150 images for each class, belonging to each classes from various provinces in Turkey. In total, deep learning-based classification and SR algorithms were applied on 900 images. In Figure 1, some of the satellite images of the data set used in this study are given. Matlab 2020a software was used to process the data divided into two main parts, training and testing for convolutional neural networks. For deep machine learning applications, MacBook Pro with an Intel i7 3.1 Ghz processor with 16 GB of RAM was used.

Figure 1. Satellite images of the data set.

The details of the SISR implementation phase used in this study are as follows.

Preparation of LR and HR Images: LR images are obtained from HR images by reducing their resolution. This reduction is typically achieved using a sub-sampling operator. Sub-sampling operators combine pixels in a known factor (e.g., 2x, 3x) to create LR images. This sub-sampling reduces the resolution of pixels based on the subsampling factor.

Image Sizes: The sizes of LR and HR images depend on the requirements of the application. Input images to have dimensions that are multiples of 2. LR image with a size of 128x128 pixels correspond to an HR image with a size of 256x256 pixels. These dimensions are important for model training and obtaining the SR output.

Data Preparation and Normalization: Data Preparation and Normalization: Images enhanced through pre-processing steps such as denoising, contrast adjustment, color space conversion, respectively. Then data normalization applied. For example, techniques like scaling pixel values to the [0, 1] range, zero-centering the mean, or unitizing the standard deviation used.

Image Feeding and Classifier Sizes: The SISR model takes LR images as input and attempts to predict HR images. In some cases, classifiers used to evaluate the quality of the SR images. The size of the images fed to classifiers depended on their specific requirements and input size constraints.

Overall, the implementation phase involves preparing LR and HR image pairs, ensuring appropriate dimensions, applying pre-processing and normalization techniques, and adapting to any specific requirements or constraints of the SISR model or associated classifiers. These steps help create an effective pipeline for generating HR images from LR inputs.

In this study, feature extraction is performed using AlexNet, ResNet50 and VGG19 pre-trained models. These models have been trained on large-scale image datasets and have learned feature representations. This typically involves resizing the image to the expected input size of the model and performing any necessary normalization or preprocessing steps. Images are given as input to the pre-trained model. Depending on the model, it extracted features from different layers. Each layer captures different levels of abstraction and represents different types of features. The features are extracted from the last convolutional layers of the algorithms. 1000 attributes were extracted from 3 architectures. The feature extraction process was applied to the images separately for without SR and with SR.

As a general approach, the available data is divided into clusters of 70% for training and 30% for testing. The training and result data of the Softmax classifier layers were extracted with Matlab software, then all images were improved over the Matlab software again for the SR method, depending on the classes. In order to prove a better classification performance by improving the satellite images of the SR algorithm, the improved images were classified with the help of convolutional neural networks after the SR step. The graphs, test times, accuracy values, complexity matrices and analysis information required for classification performance control are explained in the findings and discussion section.

First, a total of 900 image features were extracted with AlexNet, ResNet50 and VGG19 convolutional neural network architectures. Then these features are classified with classifiers such as AlexNet Softmax, ResNet50

Softmax, VGG19 Softmax, Support Vector Machine (SVM), K-Nearest Neighbor (KNN), decision trees and Naive Bayes. Resolution of the images has been increased by using SR method which has proven to perform well, which does not need the matconvnet library. SR-applied images are feature extracted with AlexNet, ResNet50 and VGG19 convolutional neural network architectures. Then these features are classified with classifiers such as AlexNet Softmax, ResNet50 Softmax, VGG19 Softmax, Support Vector Machine (SVM), K-Nearest Neighbor (KNN), decision trees and Naive Bayes. Classification performance without SR and with SR was compared. The results are explained in the findings and discussion section.

4. Experimental Results and Discussion

In this study, which aims to improve satellite images with SR, first of all, SR algorithm is applied by using satellite images. The satellite image used in the study is given in Figure 2, and the image with SR applied to the satellite image is given in Figure 3.

Figure 2. Satellite image.

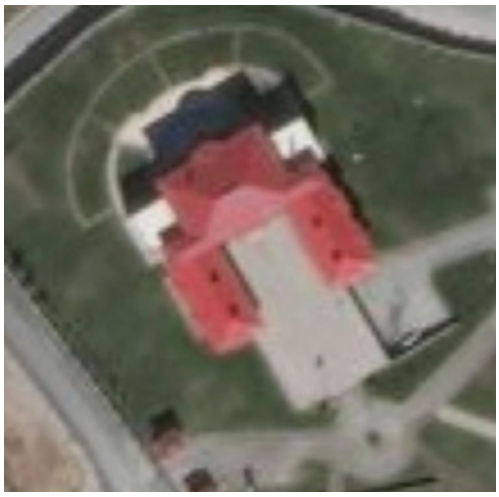

Figure 3. Image with SR applied to satellite image.

In Table 1, the peak signal-to-noise ratio (PSNR) and structural similarity index metrics (SSIM) for an image for each class of mosque, house, hospital, school, park and stadium classes used in the data set are given under the scale factor X2.

Table 1. Display Metrics.

Dataset classes	PSNR	SSIM
Data set 1	38.04	0.96
Data set 2	34.48	0.92
Data set 3	38.07	0.96
Data set 4	38.12	0.95
Data set 5	38.32	0.94
Data set 6	38.17	0.96

The satellite images were classified with deep convolutional neural networks, SVM, KNN and decision trees without SR and with SR and the results were compared. A diagram of the methods applied to satellite images is given in Figure 4.

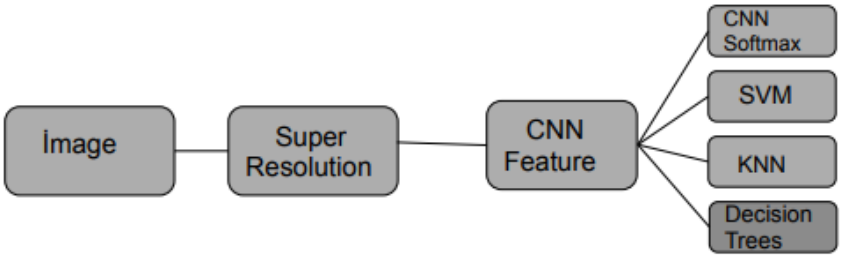

Figure 4. The diagram of the applied methods.

In another application, an accuracy of 95.6% was achieved with the softmax structure of the AlexNet convolutional neural network architecture. SR was applied to the images in order to increase the correct recognition rate. The new images obtained as a result of the SR algorithm were reclassified. Increasing the resolution of the images increased the correct recognition rate and a 97.2% success rate was achieved. Afterwards, 1000 features were extracted with AlexNet. Extracted features were given to classifiers such as SVM, KNN, Naive Bayes and Bagged Trees, and the success rates without SR and with SR were observed. All obtained results are given in Table 2 in the form of without SR and with SR. The most successful result was obtained with AlexNet-Quadratic SVM with a rate of 97.3%. 1.8% increase in performance was achieved by using SR.

Table 2. AlexNet Results.

Method	Without SR Accuracy Rates	With SR Accuracy Rates
AlexNet Softmax	95.6%	97.2%
AlexNet-Cubic SVM	94.9%	97.1%
AlexNet-Quadratic SVM	95.5%	**97.3%**
AlexNet-Linear SVM	93.5%	94.3%
AlexNet-Medium Guassian SVM	94.4%	95.8%
AlexNet-Coarse Guassian SVM	85.9%	89.3%
AlexNet-Fine KNN	90.6%	95.8%
AlexNet-Medium KNN	87.1%	88.2%
AlexNet-Coarse KNN	78.9%	81.3%
AlexNet-Cosine KNN	86.8%	87.0%
AlexNet-Cubic KNN	86.7%	88.4%
AlexNet-Weighted KNN	90.5%	93.4%
AlexNet-Subspace KNN	91.1%	95.9%
AlexNet-Bagged Trees	92.5%	89.7%
AlexNet-Kernel Naive Bayes	83.3%	85.3%

Confusion matrix of the AlexNet-Quadratic SVM method with the best classification success was created. Confusion matrix created as a result of the classification without the SR is shown in Figure 5(a) and confusion matrix created as a result of the classification with the SR is shown in Figure 5(b).

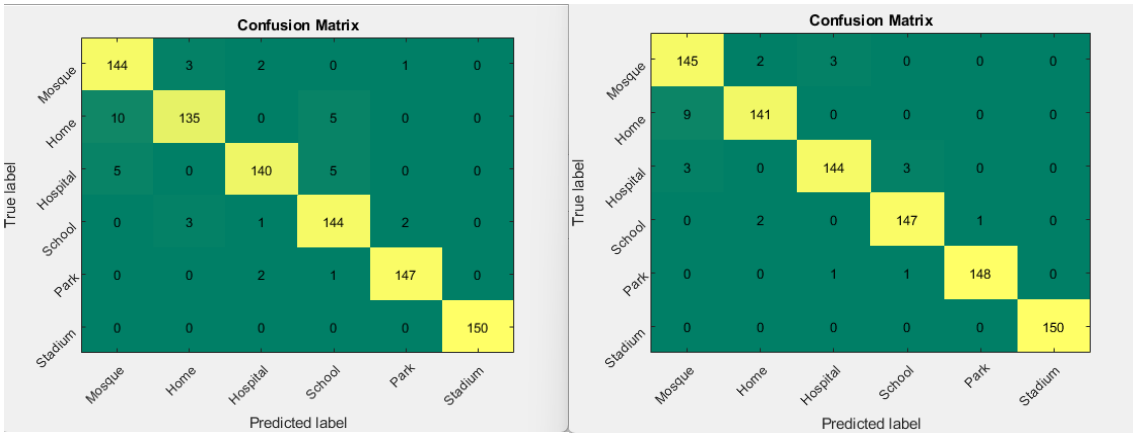

(a) (b)

Figure 5. (a) AlexNet-Quadratic SVM confusion matrix without SR (b) AlexNet-Quadratic SVM confusion matrix with SR.

In another application, an accuracy of 92.2% was achieved with the softmax structure of the ResNet50 convolutional neural network architecture. SR was applied to the images in order to increase the correct recognition rate. The new images obtained as a result of the SR algorithm were reclassified. Increasing the resolution of the images increased the correct recognition rate and a 94.1% success rate was achieved. Afterwards, 1000 features

were extracted with ResNet50. Extracted features were given to classifiers such as SVM, KNN, Naive Bayes and Bagged Trees, and the success rates without SR and with SR were observed. All obtained results are given in Table 3 in the form of without SR and with SR. The most successful result was obtained with ResNet50-Cubic SVM a rate of 98.5%. 2.2% increase in performance was achieved by using SR.

Table 3. ResNet50 Results.

Method	Without SR Accuracy Rates	With SR Accuracy Rates
ResNet Softmax	92.2%	94.1%
ResNet-Cubic SVM	96.3%	**98.5%**
ResNet-Quadratic SVM	96.3%	98.2%
ResNet-Linear SVM	94.4%	96.8%
ResNet-Medium Guassian SVM	95.6%	96.9%
ResNet-Coarse Guassian SVM	85.9%	87.9%
ResNet-Fine KNN	92.2%	96.6%
ResNet-Medium KNN	84.9%	85.0%
ResNet-Coarse KNN	69.8%	72.4%
ResNet-Cosine KNN	85.2%	86.8%
ResNet-Cubic KNN	85.2%	84.6%
ResNet-Weighted KNN	88.6%	89.3%
ResNet-Subspace KNN	92.2%	96.6%
ResNet-Bagged Trees	90.6%	94.7%
ResNet-Kernel Naive Bayes	85.1%	86.7%

Confusion matrix of the ResNet-Cubic SVM method with the best classification success was created. Confusion matrix created as a result of the classification without SR is shown in Figure 6(a) and confusion matrix created as a result of the classification with SR is shown in Figure 6(b).

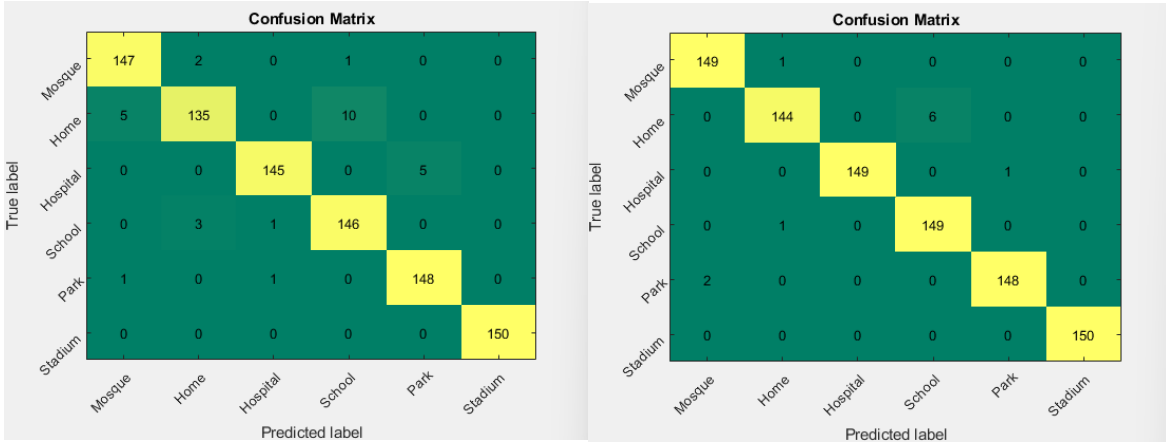

(a) (b)

Figure 6. (a) ResNet50- Cubic SVM confusion matrix without SR, (b) ResNet50- Cubic SVM confusion matrix with SR.

In another application, an accuracy of 92.2% was achieved with the softmax structure of the VGG19 convolutional neural network architecture. SR was applied to the images to increase the correct recognition rate. The new images obtained as a result of the SR algorithm were reclassified. Increasing the resolution of the images increased the correct recognition rate and a 95.2% success rate was obtained. Afterwards, 1000 features were extracted with VGG19. Extracted features were given to classifiers such as SVM, KNN, Naive Bayes and Bagged Trees, and the success rates without SR and with SR were observed. All obtained results are given in Table 4 in the form of without SR and with SR. The most successful result was obtained with VGG19-Softmax a rate of 95.2%. 3% increase in performance was achieved by using SR.

Table 4. VGG19 Results.

Method	Without SR Accuracy Rates	With SR Accuracy Rates
VGG19-Softmax	92.2%	**95.2%**
VGG19-Cubic SVM	91.7%	94.4%
VGG19-Quadratic SVM	91.7%	94.6%
VGG19-Linear SVM	89.4%	91.4%
VGG19-Medium Guassian SVM	90.8%	93.4%
VGG19-Coarse Guassian SVM	80.5%	82.2%
VGG19-Fine KNN	87.6%	91.9%
VGG19-Medium KNN	79.4%	80.9%
VGG19-Coarse KNN	65.4%	68.0%
VGG19-Cosine KNN	78.4%	81.6%
VGG19-Cubic KNN	79.8%	80.4%
VGG19-Weighted KNN	83.5%	87.9%
VGG19-Subspace KNN	87.3%	91.6%
VGG19-Bagged Trees	89.4%	92.2%
VGG19-Kernel Naive Bayes	79.4%	79.2%

Confusion matrix of the VGG19-Softmax method with the best classification success was created. Confusion matrix created as a result of the classification without SR is shown in Figure 7(a) and confusion matrix created as a result of the classification with SR is shown in Figure 7(b).

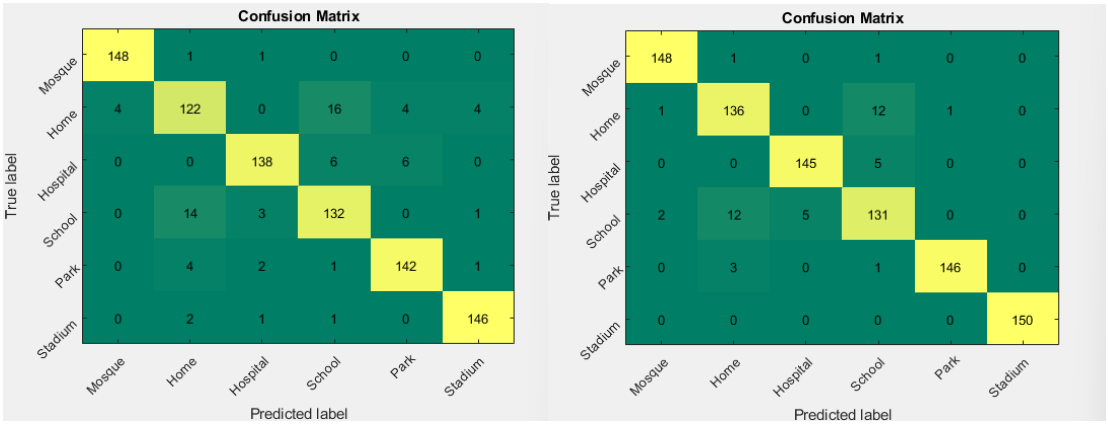

(a) (b)

Figure 7. (a) VGG19 confusion matrix without SR, (b) VGG19 confusion matrix with SR.

Table 5 shows the best results of the 3 architectures with and without SR. As a result of the applications, it has been proven that the classification success has been increased for 3 architectures. Classification performance of convolutional neural networks has increased on satellite images with SR algorithm.

Table 5. Comparison of the most successful methods.

Method	Accuracy(%)	Precision(%)	Recall(%)	F1 Score (%)	Test Time (ms)
ResNet50- Cubic SVM without SR	96.34	96.42	96.34	96.38	0.78684
ResNet50- Cubic SVM with SR	**98.50**	98.48	98.50	98.49	0.82138
AlexNet-Quadratic SVM without SR	95.54	95.57	95.53	95.55	0.50285
AlexNet-Quadratic SVM with SR	**97.33**	97.35	97.33	97.34	0.42922
VGG19-Softmax without SR	92.23	92.32	92.24	92.28	0.91659
VGG19-Softmax with SR	**95.17**	95.15	95.17	95.16	0.88269

5. Conclusion

Since the resolution of satellite images is low, the success rate in the classification process is low. In this study, SR method is proposed to increase the classification performance of satellite images. The attributes of satellite images were extracted using ResNet50, Vgg19 from deep learning architecture. Then, extracted features are divided into 6 classes by giving input to AlexNet-Softmax, ResNet50-Softmax, Vgg19-Softmax, SVM, KNN and Naive Bayes classification algorithms. without SR and with SR feature extraction and classification processes were performed separately. Classification results without SR and with SR were compared. Improvement in classification performance was observed using SR.

In this study, it is aimed to apply SR algorithms to satellite images and to increase classification accuracy by classifying images with convolutional neural network architectures. With the comparison of the applications in the study, while the success rate for ResNet50 architecture was 96.3%, it was 98.5% with SR. While the success rate for AlexNet architecture was 95.5%, it was 97.3% with SR. While the success rate for the VGG19 architecture was 92.2%, it was 95.2% with SR. In Table 5, the accuracy rates and test times of the best classifications among the classification architectures applied to the images, and the SR accuracy rates, and SR test times obtained after applying SR to the images are given. The highest accuracy rate was calculated as 97.3% for ResNet50- Cubic SVM. As seen in the applied convolutional neural networks, the accuracy values increased with the SR process. As a result of the applications, it has been proven that the classification success has been increased for 3 architectures. Classification performance of convolutional neural networks has increased on satellite images with SR algorithm.

References

[1] Dong C, Loy C, He K, Tang X. Image super-resolution using deep convolutional networks. EEE Trans Pattern Anal Mach Intell. 2015; 38(2): 295-307.

[2] Chen H, He X, Qing L, & Teng Q. Single image super-resolution via adaptive transform-based nonlocal self-similarity modeling and learning-based gradient regularization. IEEE Trans Multimedia 2017; 19(8): 1702-1717.

[3] Chang K, Zhang X, Ding P. L. K, Li B. Data-adaptive low-rank modeling and external gradient prior for single image super-resolution. J Signal Process Syst 2019; 161: 36-49.

[4] Li T, Dong X, Chen H. Single image super-resolution incorporating example-based gradient profile estimation and weighted adaptive p-norm. Neurocomputing 2019; 355: 105-120.

[5] Li J, Guan W. Adaptive lq-norm constrained general nonlocal self-similarity regularizer based sparse representation for single image super-resolution. Inf Fusion 2020; 53: 88-102.

[6] Huang J. J, Liu T, Luigi Dragotti P, Stathaki T. SRHRF+: Self-example enhanced single image super-resolution using hierarchical random forests. In Proceedings of the IEEE Conference on Computer Vision and Pattern Recognition Workshops; 2017; London. (pp. 71-79).

[7] Huang J. B, Singh A, Ahuja N. Single image super-resolution from transformed self-exemplars. In Proceedings of the IEEE conference on computer vision and pattern recognition; 2015; (pp. 5197-5206).

[8] Xiong Z, Xu D, Sun X, Wu F. Example-based super-resolution with soft information and decision. IEEE Trans Multimedia 2013; 15(6): 1458-1465.

[9] Huang J. B, Singh A, Ahuja N. Single image super-resolution from transformed self-exemplars. In Proceedings of the IEEE conference on computer vision and pattern recognition; 2015; (pp. 5197-5206).

[10] Luo J, Sun X, Yiu M. L, Jin L, Peng X. Piecewise linear regression-based single image super-resolution via Hadamard transform. Inf Sci 2018; 462: 315-330.

[11] Zhang Y, Du Y, Ling F, Li X. Improvement of the example-regression-based super-resolution land cover mapping algorithm. IEEE Geosci Remote Sens Lett 2015; 12(8): 1740-1744.

[12] Liu T, De Haan K, Rivenson Y, Wei Z, Zeng X, Zhang Y, Ozcan A. Deep learning-based super-resolution in coherent imaging systems. Sci Rep 2019; 9(1): 1-13.

[13] Jiang J, Wang C, Liu X, Ma J. Deep learning-based face super-resolution: A survey. ACM Comput Surv 2021; 55(1): 1-36.

[14] Lim B, Son S, Kim H, Nah S, Mu Lee K. Enhanced deep residual networks for single image super-resolution. In Proceedings of the IEEE conference on computer vision and pattern recognition workshops; 2017; (pp. 136-144).

[15] Hatvani J, Horváth A, Michetti J, Basarab A, Kouamé D, Gyöngy M. Deep learning-based super-resolution applied to dental computed tomography. IEEE Trans Radiat Plasma Med Sci 2018; 3(2): 120-128.

[16] Singh A, Singh J. Content adaptive single image interpolation based Super Resolution of compressed images. Int J Electr Comput Syst Eng 2020; 10(3): 3014-3021.

[17] Zhou F, Yang W, Liao Q. Interpolation-based image super-resolution using multisurface fitting. IEEE Trans Image Process 2012; 21(7): 3312-3318.

[18] Mahmoudzadeh A. P, Kashou N. H. Interpolation-based super-resolution reconstruction: effects of slice thickness. J Med Imaging Health Inf 2014; 1(3): 034007-034007.

[19] Zhang L, Zhang W, Lu G, Yang P, Rao Z. Feature-level interpolation-based GAN for image super-resolution. Pers Ubiquitous Comput 2022; 26(4): 995-1010.

[20] Gulzar S, Arora S. Optical Flow Video Frame Interpolation Based MRI Super-Resolution. In Machine Intelligence and Smart Systems; 2022; Springer, Singapore. (pp. 451-462).

[21] Alao H, Kim J. S, Kim T. S, Oh J, Lee K. Interpolation based Single-path Sub-pixel Convolution for Super-Resolution Multi-Scale Networks. Multimedia Syst 2021; 8(4): 203-210.

[22] Nazeri K, Thasarathan H, Ebrahimi M. Edge-informed single image super-resolution. In Proceedings of the IEEE/CVF International Conference on Computer Vision Workshops ; 2019; (pp. 1-10).

[23] Zope A, Inamdar V. Edge Enhancement for Image Super-Resolution using Deep Learning Approach. 2nd Global Conference for Advancement in Technology (GCAT); 2021; Bangalore, India. (pp. 1-4).

[24] Zhou W, Wang Z, Chen Z. Image super-resolution quality assessment: Structural fidelity versus statistical naturalness. 13th International Conference on Quality of Multimedia Experience (QoMEX); 2021; (pp. 61-64).

[25] Jia S, Han B, Kutz J. N. Example-based super-resolution fluorescence microscopy. Sci Rep 2018; 8(1): 1-8.

[26] Robey A, Ganapati V. Optimal physical preprocessing for example-based super-resolution. Opt Express 2018; 26(24): 31333-31350.

[27] Yang Q, Zhang Y, Zhao T. Example-based image super-resolution via blur kernel estimation and variational reconstruction. Pattern Recognit Lett 2019; 117: 83-89.

[28] Glasner D, Bagon S, Irani M. Super-resolution from a single image. 12th international conference on computer vision; 2009; Kyoto. (pp. 349-356).

[29] Timofte R, De Smet V, Van Gool L. Anchored neighborhood regression for fast example-based super-resolution. In Proceedings of the IEEE international conference on computer vision; 2013; Sydney, Australia. (pp. 1920-1927).

[30] Gao X, Zhang K, Tao D, Li X. Joint learning for single-image super-resolution via a coupled constraint. IEEE Trans Image Process 2011; 21(2): 469-480.

[31] Cheong J. Y, Park I. K. Deep CNN-based super-resolution using external and internal examples. IEEE Signal Process Lett 2017; 24(8): 1252-1256.
[32] Wang Z, Wang Z, Chang S, Yang J, Huang T. A joint perspective towards image super-resolution: Unifying external-and self-examples. In IEEE Winter Conference on Applications of Computer Vision ; 2014; USA. (pp. 596-603).
[33] Nasrollahi K, Moeslund T. B, Super-resolution: a comprehensive survey. Mach Vision Appl 2014; 25(6) :1423-1468.
[34] Chaudhuri S. Super-resolution imaging. London: Kluwer Academics Publishers, 2001.
[35] Yang W, Zhang X, Tian Y, Wang W, Xue J. H, Liao Q. Deep learning for single image super-resolution: A brief review. IEEE Trans Multimedia 2019; 21(12): 3106-3121.
[36] Wang Z, Chen J, Hoi S. C. Deep learning for image super-resolution: A survey. IEEE Trans Pattern Anal Mach Intell 2020; 43(10): 3365-3387.
[37] Jiang J, Wang C, Liu X, Ma J. Deep learning-based face super-resolution: A survey. ACM Comput Surv 2021; 55(1): 1-36.
[38] Li Y, Sixou B, Peyrin F. A review of the deep learning methods for medical images super resolution problems. IRBM 2021; 42(2): 120-133.
[39] Coşkun M, Yıldırım Ö, Uçar A, Demir, Y. An overview of popular deep learning methods. European Journal of Technique 2017; 7(2): 165-176.
[40] Dong C, Loy C. C, He K, Tang X. Learning a deep convolutional network for image super-resolution. In Computer Vision–ECCV 2014: 13th European Conference; 2014; Zurich. (pp. 184-199).
[41] Kim J, Lee J. K, Lee K. M. Accurate image super-resolution using very deep convolutional networks. In Proceedings of the IEEE conference on computer vision and pattern recognition; 2016; (pp. 1646-1654).
[42] Goodfellow I, Bengio Y, Courville A. Deep learning.London: MIT press,2016.
[43] Fu Y, Liang Z, You S. Bidirectional 3d quasi-recurrent neural network for hyperspectral image super-resolution. IEEE J Sel Top Appl Earth Obs Remote Sens 2021;14: 2674-2688.
[44] Chang Y, Luo B. Bidirectional convolutional LSTM neural network for remote sensing image super-resolution. J Remote Sens 2019; 11(20): 2333.
[45] Zhu H, Xie C, Fei Y, Tao H. Attention mechanisms in CNN-based single image super-resolution: A brief review and a new perspective. Electronics 2021; 10(10): 1187.
[46] Fu K, Peng J, Zhang H, Wang X, Jiang F. Image super-resolution based on generative adversarial networks: a brief review. Comput Mater Continua CMC 2020; 64(3): 1977-1997.
[47] Shi W, Caballero J, Huszár F, Totz J, Aitken A. P, Bishop R, Wang Z. Real-time single image and video super-resolution using an efficient sub-pixel convolutional neural network. In Proceedings of the IEEE conference on computer vision and pattern recognition; 2016; (pp. 1874-1883).
[48] Yue Y, Cheng X, Zhang D, Wu Y, Zhao Y, Chen Y, Zhang Y. Deep recursive super resolution network with Laplacian Pyramid for better agricultural pest surveillance and detection. Comput Electron Agric 2018;150: 26-32.
[49] Goyal B, Lepcha D. C, Dogra A, Wang S. H. A weighted least squares optimisation strategy for medical image super resolution via multiscale convolutional neural networks for healthcare applications. Complex Intell Syst 2022; 8:3089-3104.
[50] Zhang H, Wang P, Jiang Z. Nonpairwise-trained cycle convolutional neural network for single remote sensing image super-resolution. IEEE Trans Geosci Remote Sens 2020; 59(5): 4250-4261.
[51] Yang C. Y, Ma C, Yang M. H. Single-image super-resolution: A benchmark. In Computer Vision–ECCV 2014 13th European Conference; 2014; Zurich. (pp. 372-386).
[52] Chen H, He X, Qing L, Wu Y, Re C, Sheriff R. E, Zhu C. Real-world single image super-resolution: A brief review. Inf Fusion 2022; 79:124-145.
[53] Deng X. Enhancing image quality via style transfer for single image super-resolution. IEEE Signal Process Lett 2018; 25(4): 571-575.
[54] Zamzmi G, Rajaraman S, Antani S. Accelerating super-resolution and visual task analysis in medical images. Adv Nat Appl Sci 2020; 10(12): 1-16.
[55] Wagner L, Liebel L, Körner M. Deep Residual Learning For Single-Image Super-Resolution Of Multi-Spectral Satellite Imagery. SPRS Ann Photogramm Remote Sens Spatial Inf Sci 2019;4:189-196.
[56] Kadhim M. A, Abed M. H. Convolutional neural network for satellite image classification. Int J Intell Inf Database Syst 2020; 11: 165-178.
[57] Basu S, Ganguly S, Mukhopadhyay S, DiBiano R, Karki M, Nemani R.Deepsat: a learning framework for satellite imagery. In Proceedings of the 23rd SIGSPATIAL international conference on advances in geographic information systems; 2015; USA.(pp. 1-10).
[58] Albert A, Kaur J, Gonzalez M. C. Using convolutional networks and satellite imagery to identify patterns in urban environments at a large scale. In Proceedings of the 23rd ACM SIGKDD international conference on knowledge discovery and data mining; 2017; Canada. (pp. 1357-1366).
[59] Robinson C, Hohman F, Dilkina B. A deep learning approach for population estimation from satellite imagery. In Proceedings of the 1st ACM SIGSPATIAL Workshop on Geospatial Humanities; 2017; USA. (pp. 47-54).
[60] Unnikrishnan A, Sowmya V, Soman K. P. Deep learning architectures for land cover classification using red and near-infrared satellite images. Multimedia Tools Appl 2019; 78: 18379-18394.

[61] Özbay E, Yıldırım M. Classification of satellite images for ecology management using deep features obtained from convolutional neural network models. Iran J Comput Sci 2023; 1-9.
[62] Chen Z, Guo X, Woo P. Y, Yuan Y. Super-resolution enhanced medical image diagnosis with sample affinity interaction. IEEE Trans Med Imaging 2021; 40(5): 1377-1389.
[63] Wang P, Bayram B, Sertel E. A comprehensive review on deep learning based remote sensing image super-resolution methods. Earth Sci Rev 2022; 232:1-25.
[64] Nguyen N. L, Anger J, Davy A, Arias P, Facciolo G. Self-supervised multi-image super-resolution for push-frame satellite images. In Proceedings of the IEEE/CVF Conference on Computer Vision and Pattern Recognition; 2021; USA.(pp. 1121-1131).
[65] He Z, Li J, Liu L, He D, Xiao M. Multiframe video satellite image super-resolution via attention-based residual learning. IEEE Trans Geosci Remote Sens 2021; 60: 1-15.
[66] Agarwal A, Ratha N, Vatsa M, Singh R. Impact of Super-Resolution and Human Identification in Drone Surveillance. In 2021 IEEE International Workshop on Information Forensics and Security (WIFS); 2021; France. (pp. 1-6).
[67] Toan N. Q. Super-Resolution Method for Reconstructing Street Images from Surveillance System based on Real-ESRGAN. 8th Student Comouting Research Symposium; 2022; Slovenia. (pp.13-16).
[68] Farooq M, Dailey M. N, Mahmood A, Moonrinta J, Ekpanyapong M. Human face super-resolution on poor quality surveillance video footage. Neural Comput Appl 2021; 33(20): 13505-13523.
[69] Dabbech A, Terris M, Jackson A, Ramatsoku M, Smirnov O. M, Wiaux Y. First AI for deep super-resolution wide-field imaging in radio astronomy: unveiling structure in ESO 137-006. Astrophys J Lett 2022; 939(1): 1-22.
[70] Karwowska K, Wierzbicki D.Using Super-Resolution Algorithms for Small Satellite Imagery: A Systematic Review. IEEE J Sel Top Appl Earth Obs Remote Sens 2022; 15: 3292-3312.
[71] Ndajah P, Kikuchi H, Yukawa M, Watanabe H, Muramatsu S. SSIM image quality metric for denoised images. In Proc. 3rd WSEAS Int. Conf. on Visualization, Imaging and Simulation; 2010; (pp. 53-58).
[72] http://en.wikipedia.org/wiki/Structural_similarity, (Access date: 23.11.2022).
[73] http://www.google.com/int/tr/earth, (Access date: 16.05.2022)